*Vietnam Journal of Science and Technology* ***61*** *(6) (2023) 1010-1018*

doi:10.15625/2525-2518/16991

# Synthesis and characterization of PMMA-grafted-$ZrO_2$ hybrid nanoparticles

**Nguyen Thi Dieu Linh[1, 2], Nguyen Thi Kim Dung[3], Dam Xuan Thang[4], Do Quang Tham[1, 2, *]**

[1]*Institute for Tropical Technology, VAST, 18 Hoang Quoc Viet, Cau Giay, Ha Noi, Viet Nam*

[2]*Graduate University of Science and Technology, VAST, 18 Hoang Quoc Viet, Cau Giay, Ha Noi, Viet Nam*

[3]*National Academy of Education Management, 31 Phan Dinh Giot, Thanh Xuan, Ha Noi, Viet Nam*

[4]*Faculty of Chemical Technology, Hanoi University of Industry, Campus B5, Tay Tuu, North Tu Liem, Ha Noi, Viet Nam*

[*]Emails: *dqtham@itt.vast.vn*

Received: 14 March 2022; Accepted for publication: 26 May 2022

**Abstract.** In this study, we reported a facile synthesis and the characterization of PMMA-grafted $ZrO_2$ hybrid nanoparticles from original $ZrO_2$ ($oZrO_2$) nanoparticles. The synthesis process included of three steps: (i) modification of nano $ZrO_2$ with a vinyl silane agent, (ii) graft copolymerization of methyl methacrylate (MMA) monomers and modified $ZrO_2$ ($mZrO_2$) nanoparticles, and (iii) extraction of homo PMMA to obtain the final product of PMMA-g-$ZrO_2$ ($gZrO_2$) nanoparticles. Fourier transform infrared (FTIR) spectra and thermogravimetric analysis (TGA) of $mZrO_2$, $oZrO_2$, and $gZrO_2$ indicated that the silane coupling agent was grafted onto $oZrO_2$ nanoparticles. FTIR spectra of $gZrO_2$ indicated PMMA had been successfully grafted onto the surface of $ZrO_2$ nanoparticles. Using TGA method, the PMMA grafting content onto $ZrO_2$ nanoparticles was evaluated as 9.03 wt.%. The electron microscopy (SEM) images of $gZrO_2$, $mZrO_2$, and $oZrO_2$ indicated that their primary particle size and shape were almost unchanged after modification processes, their particle size was in the range from 50 nm to 140 nm. XRD analysis showed the monoclinic crystalline structure of three kinds of $ZrO_2$ nanoparticles (nanocrystals). The organic $gZrO_2$ nanoparticles can be a better candidate as an opacifier additive for polymer nanocomposites or acrylic bone cement.

*Keywords:* nanocrystals, grafting yield, PMMA-grafted $ZrO_2$, hybrid, graft polymerization.

*Classification numbers:* 2.4.2, 2.4.3, 2.7.1.

## 1. INTRODUCTION

Zirconia has been largely used in many technological fields because of its excellent chemical and physical properties such as chemical resistance, good mechanical strength, natural

color, low thermal conductivity, good thermal stability, corrosion resistance, and microbiological resistance [1 - 4]. First proposal for applying zirconia in medicine was made in 1969, to use it as a new material for hophead replacement instead of titanium or alumina prostheses [5]. In vitro evaluation confirmed that $ZrO_2$ is not cytotoxic [6 - 8]. Covacci *et al.* [9] and Silva *et al.* [10] had evaluated the mutagenicity and biological reactivity of zirconia and zirconia-hydroxyapatite composites ($ZrO_2$/HA), respectively. They both verified that zirconia or $ZrO_2$/HA can be safely used in biomedical applications from the point of view of low radioactive impurity content and cytotoxicity [9, 10]. Due to its great opacity, anti-shrinkage, and high hardness, zirconia is now known as an important additive in denture base resins and acrylic bone cement [11]. In these applications, zirconia is commonly used at high contents, causing an agglomeration in the polymer or resin matrices, reducing some properties of the zirconia based composite systems. Therefore, there have been studies performed on the organic modification of $ZrO_2$ nanoparticles in order to improve the compatibility and the dispersibility of $ZrO_2$ nanoparticles in polymer matrices. In the literature, several studies have used silane coupling agents to functionalize the surface characteristics of $ZrO_2$ before preparing $ZrO_2$/polymer nanocomposites [12, 13].

Recently, organic-inorganic hybrid nanocomposites have received much attention, because, these materials can combine the useful properties of organic and inorganic components that cannot be realized with single ones [14]. Pu *et al*. [15] synthesized $ZrO_2$/polymer nanocomposites by inductively coupled plasma polymerization. Sayılkan *et al*. [16] synthesized $ZrO_2$/PAAEM nanocomposites for optical purposes by hydrothermal method. Wang *et al*. prepared $ZrO_2$/PAAEM/polystyrene (PS) nanocomposites by utilizing sol-gel method and emulsifier-free emulsion polymerization. The thermal-gravimetric analysis (TGA) results indicated that the $ZrO_2$ nanoparticles had significantly improved the thermal stability of PS [17].

In this study, we propose a facile method to prepare PMMA-grafted zirconia hybrid nanoparticles followed by 3 steps: surface functionalizing of nano $ZrO_2$, synthesis of PMMA/$ZrO_2$ nanocomposite and the extraction process to obtain PMMA-g-$ZrO_2$ nanoparticles. The characterizations of the g$ZrO_2$ nanoparticles by FTIR, SEM, X-ray diffraction (XRD), and TGA were also conducted and discussed.

## 2. MATERIALS AND METHODS

### 2.1. Materials

Methyl methacrylate (MMA, 99 %, contains ~ 30 ppm MeHQ), α,α'-azobis(isobutyronitrile) (AIBN, 98 %), 3-(trimethoxysily) propyl methacrylate (MPTS, 98 %) were purchased from Sigma-Aldrich (USA). MMA was removed of the MeHQ inhibitor by passing it through a column filled with basic alumina. Nano zirconia powder ($ZrO_2$, 99.9 %), in white color with density d = 5.68 g/cm$^3$, particle size of 20 - 80 nm, was provided by Aladdins Chemical Corporation (Shanghai, China). Acetone (99.7 %), ammonia (28 %), methanol (99.7 %), ethanol (99.7 %), 1,4-dioxane (99.5 %) were the reagent grade products of Guangzhou Chemical Company, Ltd., (Guangzhou, China).

### 2.2. Sample preparation

*2.2.1. Surface modification of $ZrO_2$ nanoparticles with 3-(trimethoxysily) propyl methacrylate (MPTS) by solution method.*

Into a 500 mL round bottom flask, 100 g of nano zirconia was mixed with 200 mL methanol and 20 mL dioxane and the mixture was continuously stirred for 30 minutes. An amount of 2 mL ammonia solution (28 %) was added to adjust the pH of the solution to a value of 8.5. In a 20 mL vial, 10 g MPTS (98 %) was dissolved in methanol and water at Methanol:$H_2O$:MPTS weight ratio of 6:2:1 (MPTS/$ZrO_2$ = 0.395 mmol/g). Next, the MPTS solution was slowly injected into the bottom flask through a syringe-needle for about 2 minutes. The mixture in the flask was stirred continuously for 24 h at room temperature (from 23 - 27 °C) to allow the grafting reaction between MPTS and $ZrO_2$ nanoparticles. Residual MPTS after surface treatment was removed from the mixture by 3 cycles of centrifuging with a speed of 6000 rpm and redispersing in acetone, followed by drying in a vacuum oven at 40 °C to a constant weight. Finally, the solid part was ground by an agate pestle mortar set to obtain modified $ZrO_2$ nanoparticles (labeled as m$ZrO_2$).

*2.2.2. Synthesis of PMMA-grafted $ZrO_2$ nanoparticles*

Into a 500 mL round-bottom flask: 100 mL dioxane, 100 mL methanol, 50 gram m$ZrO_2$, 5 g MMA and 0.05 g AIBN were added, and the flask was stirred with nitrogen bubbling for 15 minutes. Next, the flask was placed in silicon oil at 60 °C. In this process, the graft polymerization reaction occurred. After 8 hours the flask was cooled down by using tap water. The PMMA-g-$ZrO_2$ nanoparticles can be easily separated from the solution containing PMMA homopolymer by using 3 cycles of centrifuging/redispersing in acetone to extract out most of the PMMA homopolymer by-product. The solid part was crushed by using an agate pestle mortar set to obtain the PMMA-g-$ZrO_2$ graft nanoparticles (labeled by g$ZrO_2$) after drying at 100 °C for 2 hours.

**2.2. Methods**

FTIR spectra of zirconia nanoparticles were performed on a Nicolet/Nexus 670 Fourier transform infrared spectrometer (Madison, WI, USA). These nanoparticles were pressed with KBr and taken IR spectra in wavenumbers ranging from 400 to 4000 $cm^{-1}$ at room temperature with 32 scans, a resolution of 4 $cm^{-1}$.

TGA and its first derivative (DTG) measurements of the o$ZrO_2$, m$ZrO_2$, g$ZrO_2$ were carried out by using a NETZSCH TG 209F1 Libra instrument (Netzsch, Munich, Germany) under nitrogen gas with a flow rate of 40 mL/min, from 30 °C to 700 °C, a heating rate of 10 °C/min and a specimen weight of about 6 - 7 mg. Grafting content and grafting yield (%) can be calculated from the TGA curves by analyzing the weight losses between 180 - 700 °C, as per described in the literature [11].

The crystalline structures of zirconia powders were examined by XRD on a Bruker-D5005 instrument (Germany) at the Institute of Chemistry and Materials, Academy of Military Science and Technology (Ha Noi).

The morphology of investigated zirconia particles was observed by using Hitachi Field Emission Scanning Electron Microscopy (FESEM, S-4800) at an electron accelerating voltage of 5 kV.

The particle size distribution of zirconia in isopropanol (at 1 wt.% solid content) was conducted via dynamic light scattering (DLS) method using a Zetasizer Ver 620 Instrument (Malvern Instruments Ltd.) with a laser light source wavelength of 532 nm at room temperature.

## 3. RESULTS AND DISCUSSION

### 3.1. FTIR spectra of $ZrO_2$, $mZrO_2$ and $gZrO_2$

The FTIR spectra of the three kinds of zirconia nanoparticles ($oZrO_2$, $mZrO_2$, and $gZrO_2$) and pristine MPTS liquid are presented in Figure 1. Figure 1a shows the stretching (ν) and bending (δ) vibrations of OH groups of zirconia at 3443 and 1626 $cm^{-1}$, respectively. The peaks at 747 and 574 $cm^{-1}$ are assigned for stretching vibrations of the Zr-O group, its bending vibration occurs at wavenumber 504 $cm^{-1}$ [18]. The FTIR spectrum of $mZrO_2$ (Figure 1b) shows the presence of the characteristic bands for MPTS, such as, ν(C=O) at 1726 $cm^{-1}$; ν(C=C) at 1633 $cm^{-1}$; δ($CH_3$) and δ($CH_2$) at 1442 $cm^{-1}$ and 1387 $cm^{-1}$, respectively. It is worthy to note that residual MPTS had almost been removed by washing and centrifuging processes. Therefore, it is reasonable to suggest that MPTS has been grafted onto the surface of $ZrO_2$ nanoparticles, as illustrated in Figure 2b.

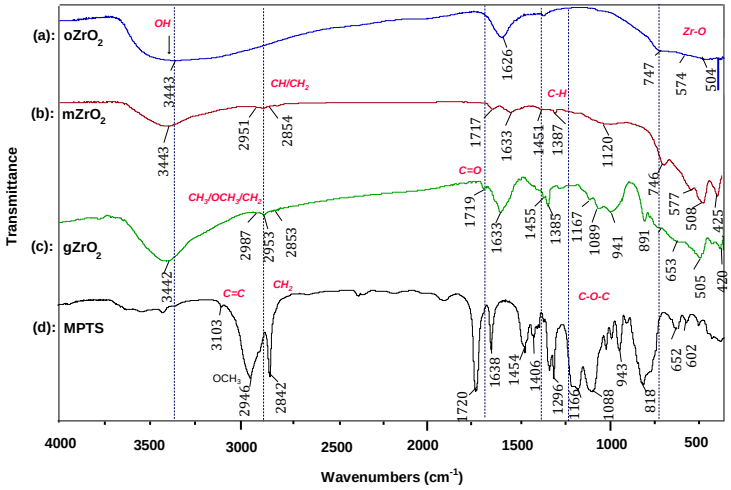


*Figure 1.* FTIR spectra (a) $oZrO_2$, (b) $mZrO_2$, (c) $gZrO_2$, and (d) MPTS.

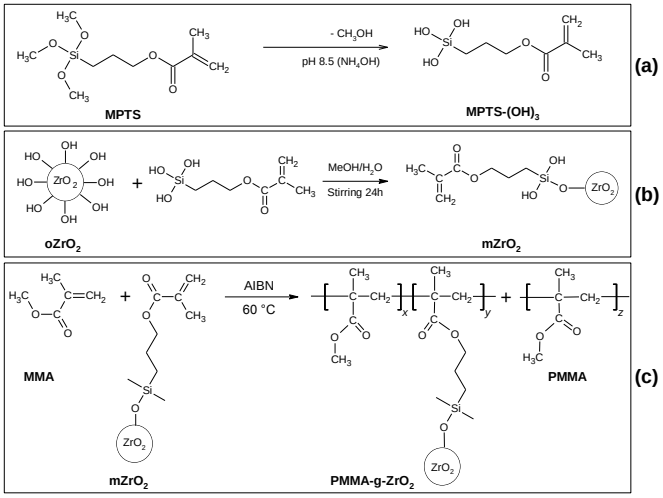


*Figure 2.* Reaction scheme of (a): MPTS hydrolysis, (b): MPTS grafting onto $ZrO_2$ nanoparticle and (c): the formation of PMMA-g-$ZrO_2$ hybrid nanoparticle.

Figure 1c is the spectrum of the $gZrO_2$, which clearly shows the specific absorption bands of the PMMA grafted onto surfaces of the $ZrO_2$ particles, such as ν(C=O) at 1719 $cm^{-1}$, ν(–$CH_3$, $OCH_3$, and $CH_2$) vibrations at 2987, 2953 and 2853 $cm^{-1}$, δ($CH_3$) at 1455 $cm^{-1}$, ν(C-O) at 1167 $cm^{-1}$, ν(O-C-Si) at 1089 $cm^{-1}$. The above results indicate that organic moieties vinyl groups and PMMA are attached to $ZrO_2$ particles. This can be explained by the reaction diagrams presented in Figure 2c which show the grafting reaction via the copolymerization of MMA and the vinyl groups on the surface of MPTS-modified $ZrO_2$ nanoparticles. As a result, PMMA molecules were formed surrounding the $ZrO_2$ particle. In this case, homo PMMA was also formed, however, this homopolymer was almost removed by the extraction process.

### 3.2. FESEM images and DLS diagrams of $ZrO_2$, $mZrO_2$ and $gZrO_2$

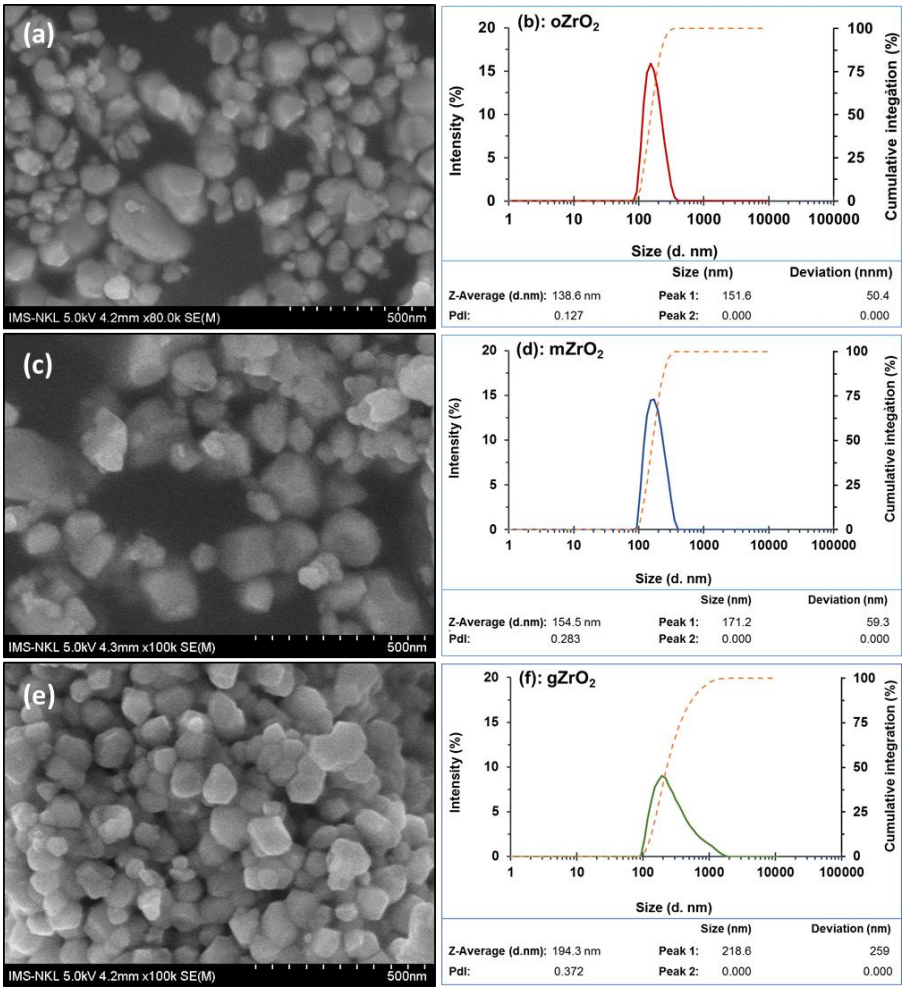


*Figure 3.* FESEM images and DLS diagrams of (a, b): $oZrO_2$, (c, d): $mZrO_2$, (e, f): $gZrO_2$, respectively.

Figure 3 presents the FESEM images and DLS patterns of 3 kinds of $ZrO_2$ nanoparticles. The FESEM images (Figures 3a, 3c, 3e) all demonstrate that the zirconia nanoparticles have a size in the range from 50 to 140 nm with the nanocrystal morphology. The size and shape of the $mZrO_2$ particles after modification are similar to the original $oZrO_2$ nanoparticles. From the FESEM image and DLS diagram of $gZrO_2$ nanoparticles (Figures 3.e and 3.f.), it can be

suggested that the zirconia particles are cross-linked together through PMMA molecular to form clusters, each cluster comprised of several $ZrO_2$ primary nanoparticles.

DLS diagrams in Figures 3b and 3d show that the particle size distributions of $oZrO_2$ and $mZrO_2$ nanoparticles are in the range of 80 - 300 with relatively low polydispersity indexes (PdI) of 0.127 and 0.283, respectively. Meanwhile, the particle size distribution of $gZrO_2$ (Figure 3f) is in a wider range (80 - 1800 nm) with higher PdI (0.372). The Z-average size of $oZrO_2$, $mZrO_2$, and $gZrO_2$ are 138,6 nm, 154,5 nm, and 194.3 nm, respectively [19]. These values are higher than those observed by FESEM. This is a common phenomenon because Z-average is a measurement of hydrodynamic particle size, while FESEM is a direct visual of particle size [20 - 23].

### 3.3. XRD patterns of $ZrO_2$, $mZrO_2$ and $gZrO_2$

Figure 4 displays the XRD patterns of $oZrO_2$, $mZrO_2$ and $gZrO_2$ samples, which indicate the same diffraction peaks at 2θ angles: 17.42, 24.04, 28.16, 31.46, 34.2, 35.32, 40.72, 45.52, 49.26, 50.10, 54.10, 55.44, 59.94, 62.88 (deg). These XRD patterns are all fitted well with ICCD 00-037-1484 standard card for monoclinic zirconia or baddeleyite crystalline with lattice constants as α = γ = 90°; β = 99.2°; a = 5.213Å; b= 5.147Å; c = 5.15Å, corresponding to lattice faces: (100), (011), (111), (-111), (002), (200), (211), (202), (022), (220), (-202), (013), (-131), (-311). This means that the organic treatment of $ZrO_2$ with MPTS or grafting PMMA does not make any change to the crystalline structure of $ZrO_2$.

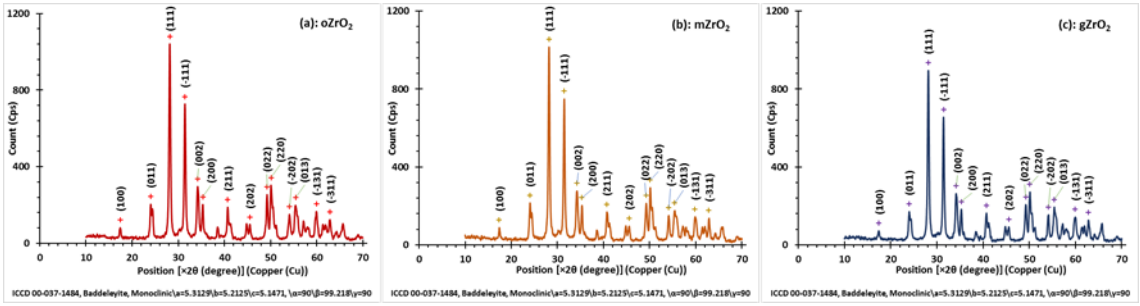


*Figure 4.* XRD patterns of (a): $oZrO_2$, (b): $mZrO_2$, and (c): $gZrO_2$.

### 3.4. Grafting yield and grafting mass of MPTS and PMMA onto the surface of $ZrO_2$

Figure 5 displays the TGA and DTG curves of $oZrO_2$, $mZrO_2$, and $gZrO_2$ samples in the temperature range from 30 to 700 °C, showing the two main stages of thermal decomposition. The first stage (I) occurs minorly from 30 °C to 180 °C with low weight loss that is attributed to the physical adsorption of water. The second stage (180 °C – 700 °C) is mainly the decomposition of organic molecules that are covalently bonded to the $ZrO_2$ nanoparticles. The grafted contents of MPTS on the surface of $ZrO_2$ nanoparticles can be evaluated from TGA measurement data as follows. Hydrolyzed MPTS has a molecular weight $M_{MPTS}$ = 248.27 g/mol, the loading amount of MPTS is 10 gram MPTS (98 %) for 100 gram $oZrO_2$ (0.395 mmol/g). The molecular weight of MPTS after hydrolysis $M'_{MPTS}$ is 206.27. Thus, the weight percentage of MPTS grafting can be calculated as 2.50 wt.% (Equation 3), and the MPTS grafting yield is 31.4 % ((Equation 4) [18].

$$\Delta m = 2.945\ \% - 0.3822\ \% = 2.554\ \% \qquad (1)$$

$$\text{MPTS grafting content in mol} = \frac{\Delta \text{ TS}}{206.27} \times 1000 = \frac{25.54}{206.27} = 0.124 \left(\frac{\text{mmol}}{\text{g}}\right) \quad (2)$$

$$\text{MPTS grafting mass} = \frac{0.124 \times M'_{MPTS}/1000}{0.124 \times M'_{MPTS}/1000 + 1} = \frac{0.0256}{1.0256} = 2.50 \text{ wt.\%} \quad (3)$$

$$\text{MPTS grafting yield} = \frac{\text{MPTS grafting content}}{\text{MPTS loading}} = \frac{0.124}{0.395} = 31.4 \text{ \%} \quad (4)$$

For the decomposition of $gZrO_2$, its TGA curve also shows the 2 stages. The first stage is also due to physical water evaporation and the second stage can be attributed to the decomposition of organic MPTS and PMMA, in which the amount of MPTS can be neglected in comparison with that of PMMA. As mentioned in section 2.2.2, the homo PMMA was almost removed through the extraction process. Therefore, the difference of weight changes between 180 - 700 °C of TGA curve $gZrO_2$ (11.97 wt.%) and $mZrO_2$ (2.945 wt.%) can be attributed to the grafted PMMA content in PMMA-g-$ZrO_2$ as described in Figure 2c. The grafted PMMA content is then calculated as 11.97 – 2.945 = 9.03 wt.% (Figure 5a) [13].

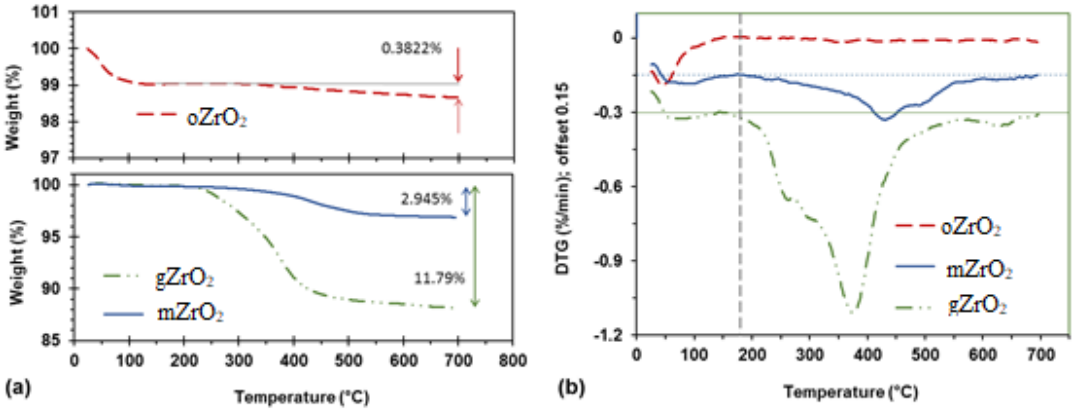


*Figure 5.* (a): TGA curves and (b) DTG curves of $oZrO_2$, $mZrO_2$, $gZrO_2$.

## 4. CONCLUSIONS

MPTS-modified and PMMA-grafted $ZrO_2$ nanoparticles ($mZrO_2$ and $gZrO_2$) have been synthesized by using a common method of silanization and copolymerization. By using FTIR and TGA method, the obtained results indicated that the MPTS and PMMA were grafted onto the surface of the $ZrO_2$ The grafting weight percentages of MPTS and PMMA were 2.5 and 9.03 %, respectively. The DLS patterns showed that the polydispersity index and particle size distribution of $gZrO_2$ nanoparticles were higher compared with $mZrO_2$ nanoparticles. FESEM images and XRD patterns indicated primary $ZrO_2$ nanoparticles did not change after silanization and PMMA grafting. With relatively high organic content, $mZrO_2$ and $gZrO_2$ nanoparticles will be good fillers for polymers, especially acrylic polymers.

***Acknowledgments:*** This research is funded by Vietnam Academy of Science and Technology (VAST) under grant number VAST03.05/20-21.

**CRediT authorship contribution statement.** Do Quang Tham: Conceptualization, methodology, writing-review and editing, supervision. Nguyen Thi Dieu Linh: Investigation, writing-original draft

preparation, formal analysis. Nguyen Thi Kim Dung: Investigation, writing-original draft preparation. Dam Xuan Thang: Investigation, data curation. All authors have read and agreed to the published version of the manuscript.

***Declaration of competing interest.*** The authors declare no conflicts of interest.

## REFERENCES

1. Wang B., Wilkes G. L. - New Ti-PTMO and Zr-PTMO ceramer hybrid materials prepared by the sol gel method: Synthesis and characterization, Journal of Polymer Science Part A: Polymer Chemistry **29** (1991) 905-909.
2. Rehman H. U., Sarwar M. I., Ahmad Z., Krug H., Schmidt H. - Synthesis and characterization of novel aramid-zirconium oxide micro-composites. Journal of Non-Crystalline Solids **211** (1997) 105-111.
3. Di Maggio R., Fambri L., Guerriero A. - Zirconium Alkoxides as Components of Hybrid Inorganic−Organic Macromolecular Materials, Chemistry of Materials **10** (1998) 1777-1784.
4. Di Maggio R., Fambri L., Mustarelli P., Campostrini R. - Physico-chemical characterization of hybrid polymers obtained by 2-hydroxyethyl(methacrylate) and alkoxides of zirconium, Polymer, **44** (2003) 7311-7320.
5. Heimann R. B., Lehmann H. D.- Bioceramics – A Historical Perspective*;* (2015) 1-10.
6. Dion I., Bordenave L., Lefebvre F., Bareille R., Baquey C., Monties J. R., Havlik P. - Physico-chemistry and cytotoxicity of ceramics, Journal of Materials Science: Materials in Medicine **5** (1994) 18-24.
7. Torricelli P., Verné E., Brovarone C. V., Appendino P., Rustichelli F., Krajewski A., Ravaglioli A., Pierini G., Fini M., Giavaresi G., Giardino R. - Biological glass coating on ceramic materials: in vitro evaluation using primary osteoblast cultures from healthy and osteopenic rat bone, Biomaterials **22** (2001) 2535-2543.
8. Lohmann C. H., Dean D. D., Köster G., Casasola D., Buchhorn G. H., Fink U., Schwartz Z., Boyan B. D. - Ceramic and PMMA particles differentially affect osteoblast phenotype, Biomaterials **23** (2002) 1855-1863.
9. Covacci V., Bruzzese N., Maccauro G., Andreassi C., Ricci G. A., Piconi C., Marmo E., Burger W., Cittadini A. - In vitro evaluation of the mutagenic and carcinogenic power of high purity zirconia ceramic, Biomaterials **20** (1999) 371-376.
10. Silva V. V., Lameiras F. S., Lobato Z. I. P. - Biological reactivity of zirconia–hydroxyapatite composites. Journal of Biomedical Materials Research **63** (2002) 583-590.
11. Zidan S. I. H.-Effects of Zirconia Nanoparticles on the Physico-Mechanical Properties of High-impact Heat-Cured Acrylic Resin Denture Base, The University of Manchester 2020.
12. Wang H., Xu P., Zhong W., Shen L., Du Q. - Transparent poly(methyl methacrylate)/silica/zirconia nanocomposites with excellent thermal stabilities. Polymer Degradation and Stability **87** (2005) 319-327.
13. Bao L., Li X., Wang Z., Li J. - Fabrication and characterazation of functionalized zirconia microparticles and zirconia-containing bone cement, Materials Research Express **5** (2018) 075404.

14. Otsuka T., Chujo Y. - Poly(methyl methacrylate) (PMMA)-based hybrid materials with reactive zirconium oxide nanocrystals, Polymer Journal **42** (2010) 58-65.
15. He W., Guo Z., Pu Y., Yan L., Si W. - Polymer coating on the surface of zirconia nanoparticles by inductively coupled plasma polymerization, Applied Physics Letters **85** (2004) 896-898.
16. Sayılkan F., Asiltürk M., Burunkaya E., Arpaç E. - Hydrothermal synthesis and characterization of nanocrystalline ZrO2 and surface modification with 2-acetoacetoxyethyl methacrylate, Journal of Sol-Gel Science and Technology **51** (2009) 182-189.
17. Wang J., Shi T. J., Jiang X. C. - Synthesis and Characterization of Core-shell ZrO2/PAAEM/PS Nanoparticles, Nanoscale Research Letters **4** (2008) 240.
18. Li D., Yao J., Liu B., Sun H., van Agtmaal S., Feng C. - Preparation and characterization of surface grafting polymer of ZrO2 membrane and ZrO2 powder, Applied Surface Science **471** (2019) 394-402.
19. Tham D. Q., Huynh M. D., Linh N. T. D., Van D. T. C., Cong D. V., Dung N. T. K., Trang N. T. T., Lam P. V., Hoang T., Lam T. D. - PMMA Bone Cements Modified with Silane-Treated and PMMA-Grafted Hydroxyapatite Nanocrystals: Preparation and Characterization, Polymers **13** (2021) 3860.
20. Danaei M., Dehghankhold M., Ataei S., Hasanzadeh Davarani F., Javanmard R., Dokhani A., Khorasani S., Mozafari M. R. - Impact of Particle Size and Polydispersity Index on the Clinical Applications of Lipidic Nanocarrier Systems, Pharmaceutics **10** (2018) 57.
21. International Organisation for Standardisation, 1996.
22. Pecora R. - Dynamic Light Scattering Measurement of Nanometer Particles in Liquids, Journal of Nanoparticle Research **2** (2000) 123-131.
23. Johnson C. S., Gabriel D. A. - Laser light scattering, CRC Press (2018) 177-248.